Advanced Fiber Materials (2022) 4:185–202
https://doi.org/10.1007/s42765-021-00109-4

REVIEW

Recent Progress of Electrospun Nanofibers for Zinc–Air Batteries

Yanan Hao[1] · Feng Hu[1] · Ying Chen[1] · Yonghan Wang[1] · Jianjun Xue[1] · Shengyuan Yang[2] · Shengjie Peng[1,2]

Received: 16 July 2021 / Accepted: 26 September 2021 / Published online: 29 November 2021

Abstract

As a potential electrochemical energy storage device, zinc–air batteries (ZABs) received considerable interest in the field of energy conversion and storage due to its high energy density and eco-friendliness. Nevertheless, the sluggish kinetics of the oxygen reduction and oxygen evolution reactions limit the commercial development of ZABs, so it is of great significance to develop efficient, low-cost and non-noble metal bifunctional catalysts. Electrospun one-dimensional nanofibers with unique properties such as high porosity and large surface area have great advantages on possessing more active sites, shortening the diffusion pathways for ions/electrons, and improving the kinetics via intercalation/de-intercalation processes, which endow them with promising application in the field of energy storage devices, especially ZABs. This review firstly introduces the electrospinning technique. Then, the oxygen reduction/evolution reaction triggered by electrospun nanofibers with self-supported structures are presented, followed by the application of electrospun nanofibers for liquid and flexible solid-state ZABs. Finally, the remaining challenges and research directions of ZABs based on electrospun nanofibers electrocatalysts are briefly discussed.

Graphic Abstract

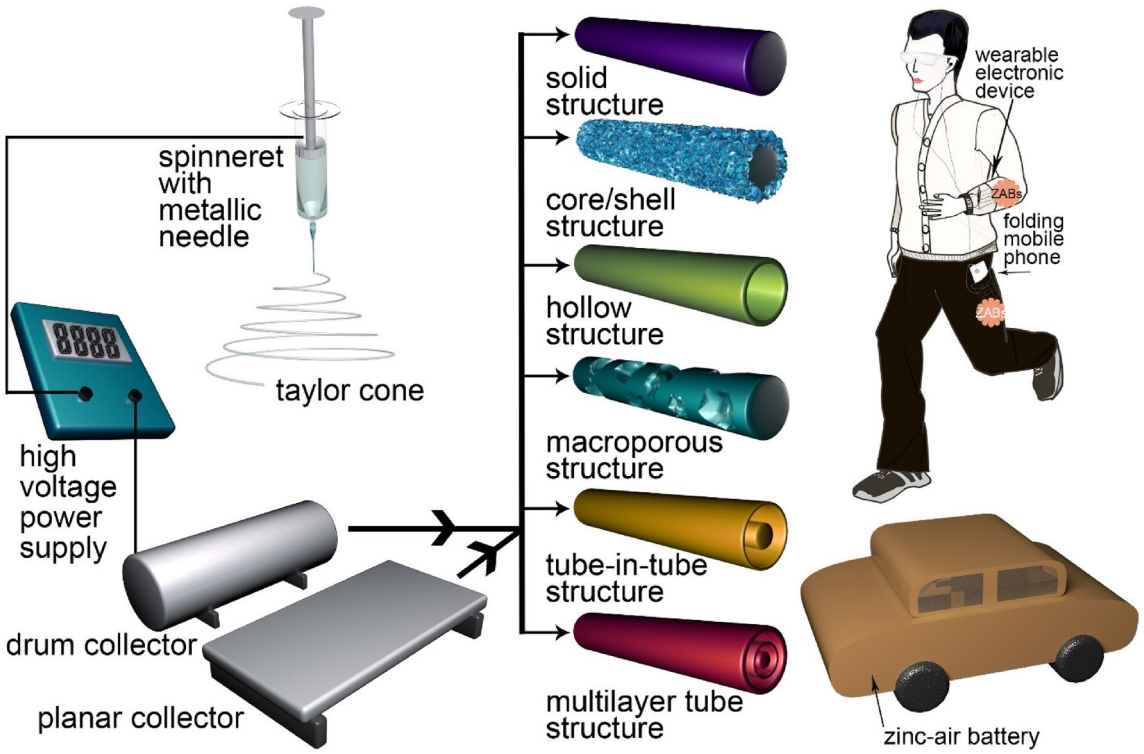

Extended author information available on the last page of the article

Keywords Electrospinning · Nanofibers · Self-supported structures · Bifunctional electrocatalysts · Zinc–air batteries

Introduction

In the past 200 years, fossil fuels including coal, oil, and natural gas have played an indispensable role as energy resources for the society. However, their excessive consumptions have exacerbated a huge outbreak of energy crisis and simultaneously caused environmental pollution. These problems have been raising the concerns of the mankind and calling for the vigorous research and deployment of sustainable and eco-environmental energy. Consequently, scientists have developed abundant, sustainable, and eco-friendly energy storage devices for the alleviation of fossil fuel consumption [1]. An extensive investigation on clean, high capacity, and renewable energy storage devices has been made, including fuel cells and metal–air batteries, which are of key importance for the diminishing non-regeneration energy consumption.

Metal–air batteries are one type of electrochemical energy storage devices, in which lithium, zinc, aluminum, sodium, and magnesium, etc., are frequently investigated as metal electrode materials [2]. Among them, the zinc electrode is more adaptable for aqueous electrolyte than other metals that are more likely to be oxidized or react with water [3]. Not only that, the zinc–air batteries (ZABs) also have an high theoretical energy density (1350 Wh kg^{-1}, excluding oxygen), which is five times more than lithium-ion batteries [4]. The advantages of high corrosion resistance in alkaline solution, large capacity, and great safety made ZABs attract augmented attentions [5, 6]. However, there are still a massive amount of scientific and technical difficulty to be solved urgently to achieve commercial applications, such as the short service life and high cost of ZABs, which are closely related to the electrocatalyst of the air electrode [7, 8]. The discharging and charging cathodic reactions of the air electrode are oxygen reduction reaction (ORR) and oxygen evolution reaction (OER) [9–11], respectively. The reaction processes of the two reactions in alkaline solutions are as shown by the equations below:

$$\text{ORR: } O_2(g) + 2H_2O(l) + 4e^- \rightarrow 4OH^-(aq), \quad (1)$$

$$\text{OER: } 4OH^-(aq) \rightarrow O^2(g) + 2H_2O(l) + 4e^-. \quad (2)$$

The efficiency of ORR and OER reactions at the air electrode are greatly limited by their sluggish kinetics involving four sequential proton-coupled electron transfer steps [12]. Generally, the catalysts of precious metal Pt and Ru can show excellent ORR and OER performances, respectively, but they can't simultaneously drive the two half-reactions of ORR and OER to achieve a lower reaction barrier in practical applications [13, 14]. In addition, the development of flexible electrodes can shorten the assembly time of ZABs and be beneficial to the application of wearable electronic devices [15, 16]. Therefore, it is particularly important to pursue a kind of low-cost, high-efficiency, and non-precious metal bifunctional electrocatalysts to meet the demand of flexible electrodes.

Structurally, the zinc–air battery consists of a zinc anode, electrolyte, and oxygen electrode. During the discharge process, the zinc anode undergoes an oxidation reaction to generate zinc ions. With the gradual accumulation of zinc ions, it begins to decompose to produce zinc oxide when the saturated concentration is reached. On the air electrode side, oxygen enters the surface of the air electrode catalyst from the external environment through the hydrophobic ventilation membrane, involving a complex four-electron reaction at the solid–liquid-gas three-phase interface to generate OH^-. Complete a complete discharge process. The charging process is a completely opposite process [4].

In terms of types, zinc–air batteries are basically divided into primary zinc–air batteries and secondary zinc–air batteries. The discharge process of a primary battery involves zinc oxidation reaction on zinc anode and oxygen reduction reaction on air cathode. When the secondary battery is charged, the reduction process on zinc anode and the air cathode oxygen evolution process during the charging process are alternatively taken place. Flexible batteries have different structures, such as sandwich structure, cable structure, book page shape, etc. The electrochemical properties can be maintained under the applied deformation, such as folding, twisting, or stretching. The other type is the cable-shaped flexible zinc–air battery [5], in which the metal electrode is in the central axis wound by the gel electrolyte. The air electrode wraps the outside of the electrolyte to form the basic structure of the flexible battery [17]. Moreover, the insulating material plays the role of encapsulation and protection on the outermost side.

Electrospinning is a versatile and simplified fiber manufacturing technique that uses polymer precursors to generate a tunable one-dimensional (1D) nanofiber structures with adjustable morphology [18–20]. To achieve the controllable preparation of adjustable morphology of electrospun nanofibers, some typical methods involve pore structure controlling (e.g., coaxial spinneret, volatility of solvent), metal loading, as well as parameter tuning of polymer solution (e.g., viscosity, electrical conductivity) and processing conditions (e.g., flow rate of solution, voltage, humidity, and temperature) [21]. The electrospun nanofibers enjoy the advantages of large surface area and high aspect ratio. Especially, the electrospun nanofibers with hollow or porous

structure via electrospinning can highlight its cross-linked channels and larger surface area, which not only provides more active sites and energy storage sites but also shortens the diffusion pathways for ions/electrons and promote ion/electrons absorption [22–24]. Higher pore volume and richer porosity of electrospun nanofibers with these unique structures further expand the contact between the electrolyte and catalyst, which facilitates improved kinetics via intercalation/de-intercalation processes of active species [25–27]. A large number of documents have reported the emergence of electrospun nanofibers as electrocatalysts, polysulfide intermediates, and high capacity electrode materials, which have elevated the electrochemical performance of energy storage devices [28, 29]. In addition to energy conversion/storage devices, electrospun nanofibers also have several novel applications in the field of medicine, such as wearable biosensors, drug delivery devices, and biomedical scaffolds [30, 31].

One critical aspect of the research about electrospun nanofibers electrocatalyst is the design of ameliorated polymer precursors and optimized process parameters to synthesize complex structures, such as solid, core/shell, hollow, porous and tube-in-tube structures. These unique structures can facilitate to expose more active sites and generate distinctive electronic structures on the surface of electrospun nanofiber electrocatalysts. Most electrospun nanofibers electrocatalysts use traditional methods to prepare powder electrode materials. However, the catalyst will peel off from the surface of the current collector, which results in poor stability. Therefore, the electrode needs a binder (Nafion, PVDF, etc.) to fix the powder catalyst by grinding. That mechanically grinding restricts the advantages of nanofibers' high aspect ratio, and irreversibly destroys the 1D morphology of the electrospun nanofibers [32]. Moreover, the addition of binders will also obstruct the active sites, constrain ion/electron diffusion and restrict the practical interaction on the electrochemical interfaces [33]. The development of electrospun nanofibers with self-supported structure breaks through the bottleneck of traditional powder catalysts that needed the addition of binders. The self-supported or free-standing structure is a steric structure with a certain spatial structure that can be used as a binder-free carrier to directly synthesize nanocatalysts in situ. The high interaction forces between the carrier and catalyst affect the growth and arrangement orientation. The catalyst is fixed under the premise of binder-free to avoid peeling off during the electrochemical reaction [34]. Self-supported structure can be divided into two categories according to the presence or absence of substrate. One is material natively in situ grown on conductive substrates (e.g., metal foam, carbon paper, carbon cloth, metal foil, metal stainless steel mesh, etc.), the other is a substrate-free gas diffusion electrode synthesized in one step, which contains the substrate itself. Electrospun nanofiber is a typical substrate-free self-supported structure. It has the following advantages, (1) easy application by directly used as working electrode; (2) strong ion/electron diffusion without high-cost binders; and (3) stable electrochemical reaction durability [17]. Electrospun nanofibers catalysts show great potential in energy applications, especially there is a multitude of research articles that have investigated the improvement of ZABs performance in the field of electrospun nanofibers catalysts. Accordingly, this paper is an explicit and focused review to generalize the application of electrospun nanofibers catalysts in ZABs [35].

This review emphasizes the recent research of electrospun 1D nanofibers that are applied to cathodic electrocatalysts of ZABs. The content covers a brief outline of the electrospinning technique, the controllable preparation of electrospun nanofibers with different structures, the comparison of electrospun nanofibers catalysts with self-supported structure and traditional powder catalysts, and the recent progress of electrospun nanofibers as cathode electrocatalysts in liquid and solid ZABs. Finally, we evaluate the challenges and deficiencies, and also look forward to an alluring promise to provide a timely and realistic cognition of this rapidly developing domain.

Electrospinning Technique

Electrospinning technique, firstly described by Zeleny in 1914 [36], has been proved to be an exceptional nanofiber preparation technique for its simplicity, effectivity, low-cost, and repeatability. This technique can generate ultrafine fibers of mm to nm scale from a sequence of different polymers, including not only non-water-soluble polymers like polyacrylonitrile (PAN), and polystyrene (PS), but also water-soluble polymers such as poly(vinyl pyrrolidone) (PVP) [21]. Electrospinning is a facile electrohydrodynamic (electrically charged fluids kinetics, the basis for forming electrospun fibers) fabrication method that can generate nanostructured fibers through tunable release dynamics, it affords near zero-order release dynamics, dampening of burst release. There is an analytical and theoretical framework for modeling the forming electrospun fibers. The properties of polymer solution and processing condition (liquid dynamic viscosity/inertia, surface charge density, and local electric field, etc.) are important for the geometry types of electrospun fibers. Due to the opposition of electrostatic repulsion and surface tension, the liquid drop exits from the capillary and deforms into a Taylor cone, then a charged jet escapes and elongates towards the collector as the voltage increases. There is a steady-state relation:

$$d = \left(\frac{Q^3\rho}{2\pi^2 E_\infty I}\right)^{\frac{1}{4}} z^{-\frac{1}{4}} \quad (3)$$

in which d represents the jet diameter, and Q, ρ, E_∞, and z correspond to the flow rate, fluid density, applied field strength, and axial coordinate, respectively [37].

The fundamental setup of electrospinning is illustrated in Fig. 1a, a spinneret with a metallic needle, a grounded planar or drum collector, and a high voltage power supply to generate an electrical field up to 3000 kV m^{-1} are essential. A classic electrospinning process involves the application of a strong electric field to a drop of the polymeric precursor solution. When a pendant fluid drips from the tip of the spinneret, a high voltage applied between the spinneret and collector electrifies a droplet and uniformly distributes charges onto the hemispherical surface. Furthermore, the interactions of the external electric field with the internal charges facilitate the formation of Taylor cone which is a conical structure. The electrostatic forces will overcome by the surface tension of the drop when the applied voltage transcends the critical voltage. Then a fine-charged jet will eject to evaporation and elongate during an unstable whipping. Finally, the solidification of ultra-fine fibers is ended on the grounded collector. Several structures, such as solid, core/shell, hollow, porous, tube-in-tube, and multilayer tube structures, would be fabricated in consequence of different parameters. For decades, due to the high pore volume, conspicuous mechanical strength, and controlled designed architecture, electrospinning has become a versatile and attracting craft. Inspired by the outstanding stability and bifunctional activity of electrospun nanofibers, we then exhibit its practical application in the flexible solid-state and liquid ZABs (Fig. 1b–d [38, 39]) which can be applied for wearable electronic watch, folding mobile phone, and zinc–air electric vehicles.

The ultimate characteristics of electrospun nanofibers are principally modulated by a wide variety of parameters such as process conditions (voltage strength, humidity, and solution feed rate), adjustable precursor solution (viscosity, concentration, categories of polymers and additive) and supplementary step (temperature and time of calcination or carbonization). Different parameters can be easily used to regulate the size (length and diameter), morphology (spheres or fibers), and structure (solid, hollow, porous, or tube-in-tube) of electrospun nanofibers, which would change their subsequent properties including their catalytic activities. Several investigations have detailed the evolution of electrospun nanofiber catalysts with unique structures.

For instance, the solid structure of nanofibers is shown in Fig. 2a [40], the interpenetrating of 1D nanofiber enabling a network morphology is better to contribute charge conduction than sintered aggregates, because of its large surface area of high aspect-ratio nanofibers for the increased adsorption of intermediates. This carboxyl-modified porous electrospun nanofiber anchored with Ni and Mn has been reported to exhibit ultra-low ORR/OER overpotential, as well as high power density and stability in their ZABs. While its appreciable electrochemical performance is attributed to the synergy of the heterogeneous interface between

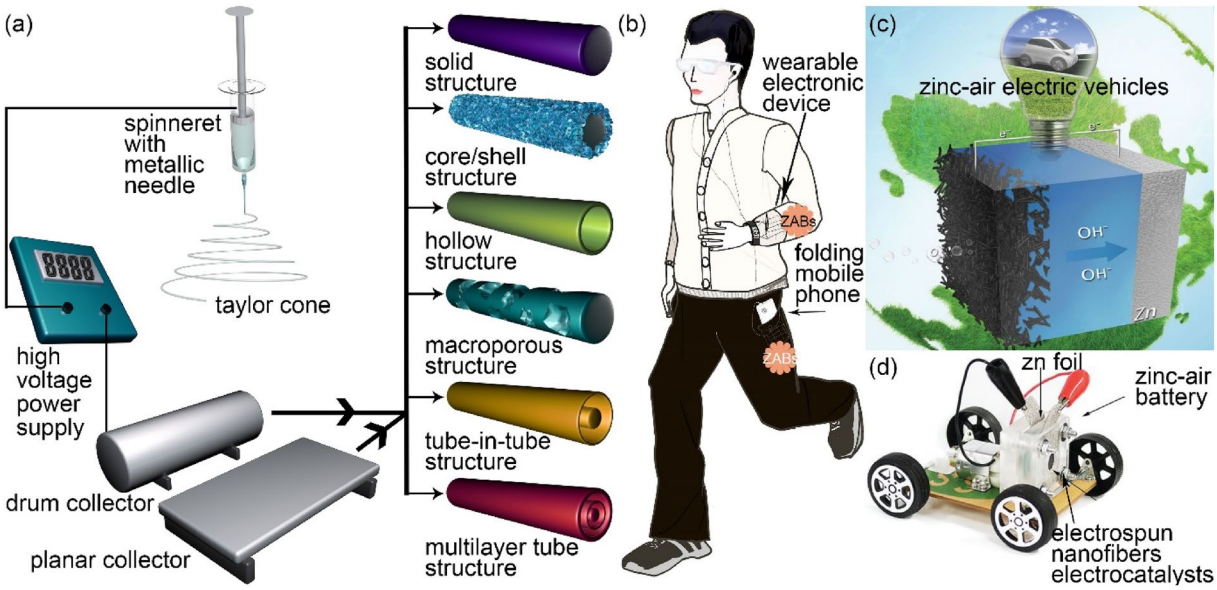

Fig. 1 **a** Schematic diagram of the fundamental setup of electrospinning to obtain ultra-fine fibers, and several structures of electrospun nanofibers. **b** Application of flexible solid-state ZABs like wearable electronic devices. **c** [38], **d** [39] Liquid ZABs based on electrospun nanofibers electrocatalysts like zinc–air electric vehicles

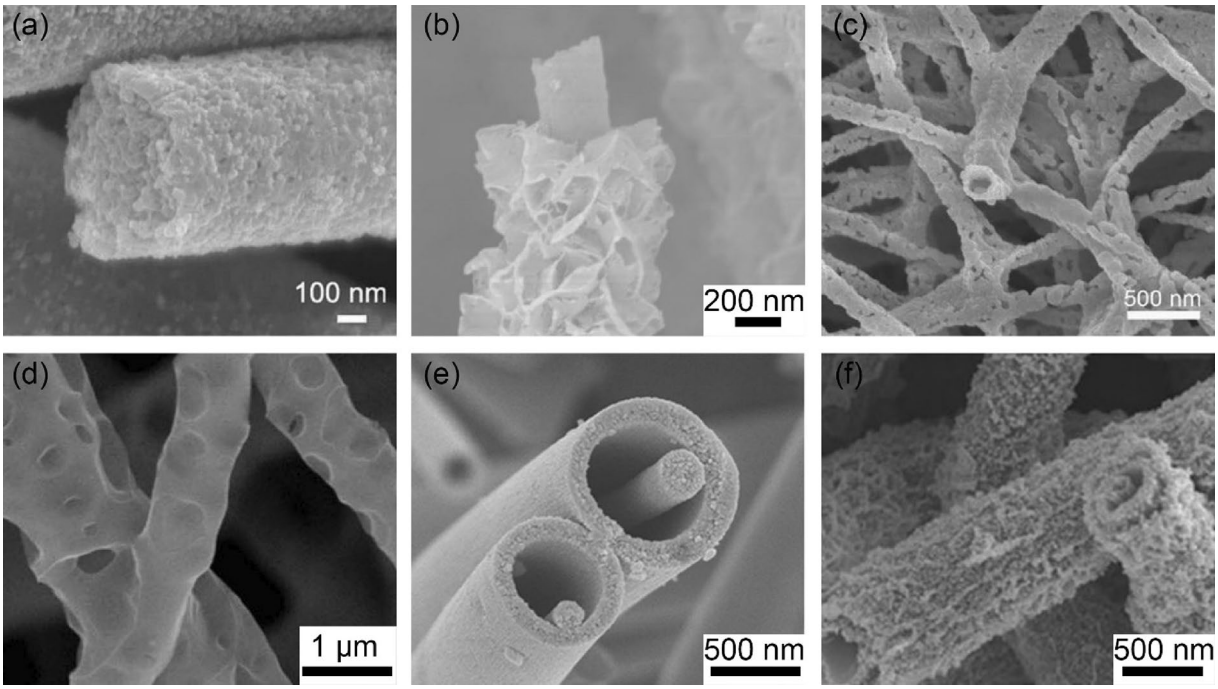

Fig. 2 SEM images of **a** solid structure [40], **b** core/shell structure [41], **c** hollow structure [42], **d** macroporous structure [43], **e** [44] and **f** [45] tube-in-tube structure of electrospun nanofibers by different operational parameters

different metals and 1D porous nanofibers. In other examples, the nanosheets, nanoparticles, and nanowires can be in situ grown on nanofiber to form the core/shell structure (Fig. 2b [41]). Research shows that the proton transports on the interfaces of sheets/particles/wires, where electrochemical reactions take place, rather than within the fiber itself. Accordingly, this structure exhibits higher conductivity compared with the counterparts of particles, sheets, or wires. In addition, complex hollow structure (Fig. 2c, [42]), and microporous structure (Fig. 2d, [43]) can be fabricated via volatile and nonvolatile polymers, which provide rapid adsorption/access of the electrolyte to the catalytic layer and promote fast charge/discharge processes and proton transport. That has been shown to be effective on optimizing the activity of catalysts. Classic instances of the hollow structures are the tube-in-tube structure (Fig. 2e, [44]), and even the multilayer tube structure (Fig. 2f, [45]). These complex structures are synthesized by a coaxial spinneret with multiple syringes. With different precursor fluids loaded in the multiple syringes, the middle fluid corresponding to the hollow part could be selectively removed while the inner and outer polymer fluids corresponding to the solid part could have remained. Compared with the solid structure, the multilayer tube structure increased surface area to expose more active sites and elevated the effective contact area with electrolyte. Therefore, the rational design of electrospun nanofiber structures could simultaneously reduce the ORR/OER reaction barrier and optimize its ZABs performance.

Electrospun Nanofibers as Bifunctional Electrocatalysts

Electrospun Nanofibers Powder Electrocatalysts

At present, there have been multiple studies on electrospun nanofibers electrocatalysts. In general, the electrochemical test of catalysts uses a three-electrode system, the working electrode of this system is prepared by a common process. First, 7 mg electrospun nanofibers catalysts was mixed with 2 mg of conductive additive (such as carbon black), and 50 μL binder (such as Nafion) and grind them into powder. Then, 760 μL of ethanol and 190 μL of DI water were added to the mixer followed by 1 h ultrasonic to form a homogeneous catalyst ink. Ultimately, the ink was dropped evenly on a pre-cleaned glassy carbon disk as a working electrode. Some typical examples about the ORR and OER performances of electrospun nanofibers powder electrocatalysts are shown in Table 1. As stated, there are many advantages of electrospun nanofibers catalysts, such as multiple activity sites, sufficient conductivity and controllable defect preparation. Furthermore, its catalyst activity is directly affected by multitude of cross-linked pores, large aspect ratio and unique hollow structure. Most electrospun nanofibers powder electrocatalysts in this table demonstrate more efficient ORR/OER activity in the field of powder catalysts. Mesoporous Fe/Co–N–C nanofibers with embedding FeCo nanoparticles (FeCo@MNC) are synthesized by a constrained-volume

Table 1 ORR and OER performances of recently reported electrospun nanofibers for powder electrocatalysts

Catalyst	E_{onset} (V)	$E_{1/2}$ (V)	$E_{j=10}$ (V)	$\Delta E = E_{j=10} - E_{1/2}$ (V)	n	References
CMO/S-300	0.915	0.760	1.700	0.940	3.91	[42]
N, F, P tri-doped carbon nanofibers	–	0.8	1.67	0.87	2.46	[43]
FeCo@MNC	–	0.86	1.47	0.61	3.87	[46]
NiCo@N-C 2	–	0.81	1.76	0.95	3.99	[47]
NiCoP/CNF nanofibers	0.92	0.82	1.498	0.678	4	[48]
AgCo composite nanotubes	0.9464	–	–	–	3.80	[49]
$Ir_{0.46}Co_{0.54}O_y$ nanotubes	–	–	1.54	–	–	[50]
Fe/N/F MCNFs	0.900	0.822	–	–	4	[51]
$NiCo_2O_4$-A_1 nanostructure	0.93	0.78	1.62	0.84	4.0	[52]
NiFe@NCNFs	–	–	1.524	–	–	[53]
$LaNi_{0.85}Mg_{0.15}O_3$	0.82	0.69	1.68	0.99	3.4	[54]
FeCo@N-GCNT-FD	0.98	0.8	–	–	4	[55]
Ru_1Ni_1-NCNFs	–	–	1.52	–	–	[56]
Pt/Ta/SnO_2	1.0	0.9	–	–	–	[57]
CNCF-800	0.83	0.66	1.64	0.98	4	[58]
Pd_3/Y-ACNF	0.90	0.81	–	–	4	[59]
Fe_3C@NCNTs-NCNFs	–	–	1.514	–	–	[60]
BSCF-80-ES	0.78	0.64	1.60	0.96	3.83	[61]
ES-CNCo-5	0.8872	0.8122	–	–	4	[62]
CNF@NC	–	0.72	–	–	4.0	[63]
Co_3O_4/N-ACCNF	0.98	0.79	1.54	0.75	4.0	[64]
50 wt% NiFe-CNF	–	–	1.50	–	–	[65]
Fe/N-CNFs	0.96	0.88	–	–	3.8	[66]
1D $Co_3V_2O_8$ nanostructures	–	–	1.58	–	–	[67]
Pt/TiN NTs	0.957	0.843	–	–	–	[68]
LSCF@$Ni_3(HITP)_2$-2	–	–	1.502	–	–	[69]
N/Fe-CG	0.93	0.73	–	–	4.0	[70]
$Pt_1Au_1/(TiO_2)_{0.5}$ NWs	1.046	0.889	–	–	3.8	[71]
$CoFe_2O_4$@N-CNFs	–	–	1.579	–	–	[72]
CMS/NCNF	0.969	0.861	1.732	0.871	4	[73]
$NiCo_2O$@C	–	0.847	1.537	0.69	3.99	[74]
CCO@C	0.951	–	1.557	–	3.9	[75]
$NeTiO_2$@C-0.75	0.9782	0.7502	–	–	3.85	[76]
FeS_2-CoS_2/NCFs	–	0.81	1.57	0.76	3.90	[77]
TCNFs/C	0.941	0.710	–	–	3.29	[78]
h-Co_3O_4/CeO_2@N-CNFs	–	–	1.54	–	–	[79]
FeCo@NCNS	0.98	0.83	1.597	0.767	3.97	[80]
$PrBa_{0.5}Sr_{0.5}Co_{2-x}Fe_xO_{5+\delta}$-NF	–	0.69	1.53	0.84	3.8	[81]
Co-N_x@CNF700	0.941	0.814	–	–	3.9	[82]
Fe_3C@MHNFs	–	0.90	–	–	4	[83]
Co-CeO_2-N-C nanofibers	0.89	0.82	1.556	0.736	3.96	[84]
FeCNFs-NP	0.9842	0.8842	1.56	0.6758	3.9	[85]
ZCP-CFs-9	–	0.8332	–	–	3.97	[86]
CMO/NCNF	1.05	0.83	1.57	0.74	3.7	[87]
$Ni_3V_2O_8$ NFs	–	–	1.562	–	–	[88]
Pt/HPCNF-1000	0.895	0.763	–	–	–	[89]
Co_2RhO_4 nanotubes	–	–	1.519	–	–	[90]
Zn/Co@C-NCNFs (0.50)	0.8682	0.7672	–	–	3.69	[91]
NSCFs/Ni-Co-$NiCo_2O$	–	0.806	1.498	0.692	3.97	[92]
FeNi/N-CPCF-950	–	0.864	1.585	0.718	3.98	[93]

Table 1 (continued)

Catalyst	E_{onset} (V)	$E_{1/2}$ (V)	$E_{j=10}$ (V)	$\Delta E = E_{j=10} - E_{1/2}$ (V)	n	References
LCNP@NCNF	0.870	0.72	1.81	1.09	–	[94]
Fe-N/$C_{air/NH}$	–	0.87	–	–	4	[95]
Co@N-PCF-$_3$	0.9212	0.8332	–	–	3.9	[96]
Co_9S_8/NSC nanofibers	–	0.84	1.56	0.72	3.54	[97]
Fe_3C@B_xNPCFs	0.968	0.832	–	–	4.00	[98]
ZIF-67/PAN-800	0.90	0.81	1.64	0.83	3.4	[99]
Fe-N-Si-CNFs	–	0.86	–	–	3.89	[100]
CoP/NC-800	0.90	0.78	1.52	0.74	3.62	[101]
MB-CFs-0.6	–	0.8172	–	–	3.95	[102]
FeCo@PCNF-800	0.939	0.854	–	–	3.99	[103]
Mo_2N-MoS_2(1:1) MCNFs	–	–	1.50	–	–	[104]
Pt–Fe/CNFs-900	0.99	0.79	–	–	4.09	[105]
FeCoP@NCNFs	–	–	1.52	–	–	[106]
Nb CNF-Pt	0.99	0.89	1.555	0.665	4	[107]
$Ni_{2-x}Co_xP$/N-C NFs	–	–	1.51	–	–	[108]
Fe1Ni1-N-CNFs	0.903	0.791	1.602	0.811	3.97	[109]
SNCF-NR	–	–	1.62	–	–	[110]
NCNF-1000	097	0.82	1.84	1.02	4.0	[111]
$La_{0.6}Sr_{0.4}Co_{1-x}Fe_xO_{3-\delta}$	–	–	1.877	–	–	[112]
CNCo-5@Fe-2	0.971	0.861	–	–	3.99	[113]
Fe-CoO/C-800	–	–	1.592	–	–	[114]
FeCo-NCNFs-800	0.907	0.817	1.686	0.869	3.91	[115]

E_{onset}, $E_{1/2}$, and n denote ORR onset, half-wave potential, and electron transfer number. $E_{j=10}$ is the required potential to reach an OER current density of 10 mA cm^{-2}

method from Fe/Co–N coordination compounds, resulting in the enhanced ORR and OER activity of FeCo@MNC ($E_{1/2}$ = 0.86 V, $E_{j=10}$ = 1.47 V) [46]. Compared with other samples in this table, FeCo@MNC has the lowest overpotential ($\Delta E = E_{j=10} - E_{1/2}$) of 0.61 V. As shown in Fig. 3a–f, such outstanding advantages benefit from the great electrical conductivity of larger aspect ratio nanofibers, multitude interconnected pores which were beneficial for O_2 speedy transportation and substantial reactive active sites exposing, thereby reducing the ORR/OER reaction barrier. Therefore, FeCo@MNC can be applied as a bifunctional electrocatalyst of ZABs for a higher power density and lower charging/discharging voltage gap.

Electrospun Nanofibers Electrocatalysts with Self-Supported Structure

The electrospun nanofibers catalysts with self-supported structures have unique mechanical properties, such as great flexibility and foldability, which fundamentally breaks the bottleneck of the powder catalysts added with the binder in the convenient process. As well known, the binder will not only retard the adsorption sites of oxygen but also inhibit ion diffusion and increase the resistance. In particular, avoiding the addition of binder allows for a degree of staving off agglomeration and pulverization of the electrode. Additionally, the air electrode based on electrospun nanofibers with self-supported structure has validly reduced the assembly time of the flexible solid-state ZABs, so the flexible electrode has been widely studied in wearable electronic devices. The current research is focused on how to prepare electrospun nanofibers with mechanical strength and toughness simultaneously, and how to drive ORR/OER to achieve a steady effective activity. The ORR and OER performances of several decent electrospun nanofibers with self-supported structure are listed and compared below in Table 2. Comparison of Tables 1 and 2 shows that the ORR/OER overpotential (ΔE) of electrospun nanofibers with self-supported structure is generally lower than powder electrospun nanofibers because they are fixed under the premise of binder-free to avoid peeling off during the electrochemical reaction. Moreover, binder-free catalysts are conducive to expose the active sites, accelerate ion/electron diffusion and promote the practical interaction on the electrochemical interfaces. These examples demonstrate that the electrospun nanofibers with self-supported structures are more suitable as bifunctional electrocatalysts with outstanding ORR/OER efficiency than electrospun nanofibers powder electrocatalysts. As shown in Fig. 4a–d [17], Co_3O_4 hollow particles with tailored oxygen vacancies (Co_3O_{4-x}HoNPs@HPNCS) are synthesized through Kirkendall effect, which emerges a lower reversible

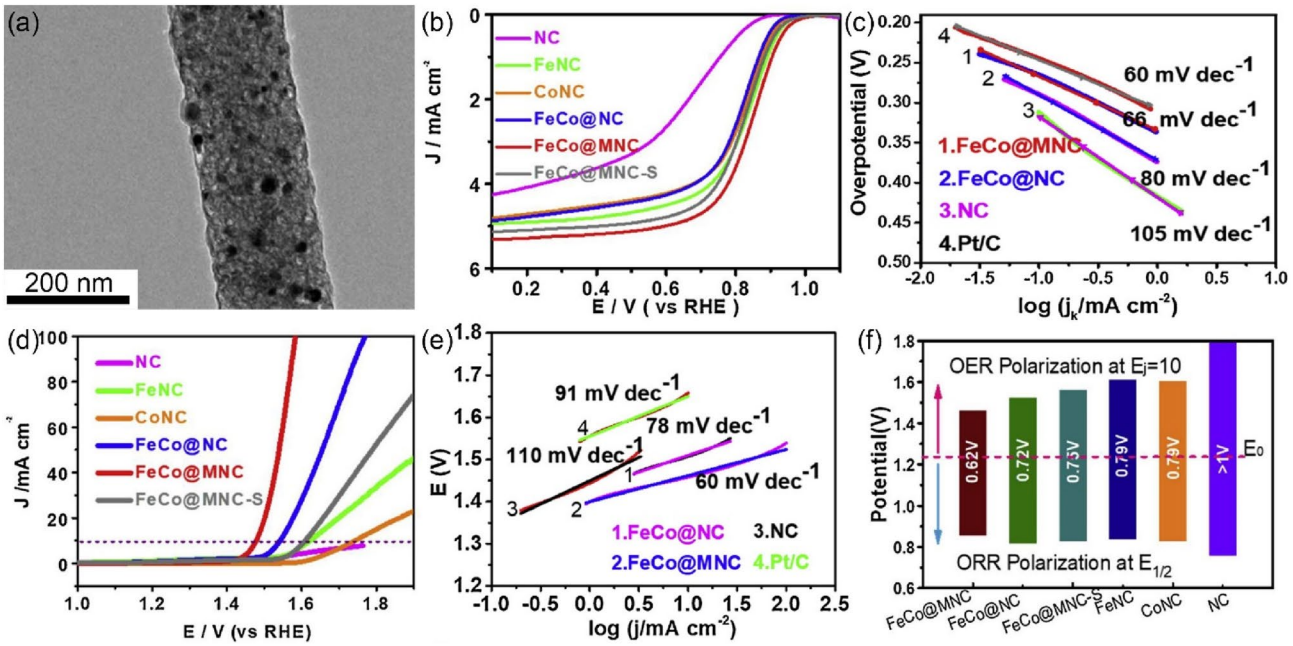

Fig. 3 **a** TEM image of FeCo@MNC. **b** ORR polarization curves of different catalysts recorded at 10 $mV{\cdot}s^{-1}$. **c** The corresponding ORR Tafel plots of different catalysts. **d** OER polarization curves of different catalysts recorded at 5 $mV{\cdot}s^{-1}$. **e** OER Tafel slopes on different catalysts. **f** The potential gap (ΔE) between the $E_{1/2}$ of ORR and $E_{j=10}$ of OER for different catalysts [46]

Table 2 ORR and OER performances of recently reported electrospun nanofibers electrocatalysts with self-supported structure

Catalyst	E_{onset} (V)	$E_{1/2}$ (V)	$E_{j=10}$ (V)	$\Delta E = E_{j=10} - E_{1/2}$ (V)	n	References
Ni|MnO/CNF	–	0.83	1.58	0.763	4.0	[40]
$CuCo_2S_4$ NSs@N-CNFs	0.957	0.821	1.545	0.751	3.99	[41]
Co_3O_{4-x} HoNPs@HPNCS-60	–	0.834	1.574	0.74	4.0	[17]
Ni@PIM-CF	–	–	1.62	–	–	[116]
CoNCNTF/CNF	0.974	0.857	1.61	0.76	3.9	[117]
CoZn-ZIF-500	–	–	1.575	–	–	[118]
AgNF networks	1.041	0.848	–	–	4	[119]
PdNi/CNFs-1:2	–	–	1.519	–	–	[120]
Co SA@NCF/CNF	–	0.88	1.63	0.75	4.0	[34]

overpotential (ΔE = 0.74 V). Benefiting from the building of a flexible self-supporting structure, this kind of electrospun nanofibers electrocatalysts as air electrode can shorten the path of ion diffusion and improve the electron transmission rate, which will improve the ORR and OER reaction kinetics.

Electrospun Nanofibers for ZABs

Liquid ZABs Based on Electrospun Nanofibers Electrocatalysts

A schematic configuration of rechargeable liquid ZABs is shown in Fig. 5a, in which a rechargeable ZAB includes zinc foil (anode), a gas diffusion electrode (cathode), and electrolyte (such as 6.0 M KOH/0.2 M $ZnCl_2$). The gas diffusion electrode contains gas diffusion layer (GDL, which could accelerate the adsorption/desorption of O_2 for the ORR/OER process and prevent electrolyte loss), current collector layer (gather and conduct electrons) and catalytic layer (the place where ORR and OER react). Thanks to the promising advantages of cross-linked porous, large surface area, and high porosity, the electrospun nanofibers are generally used in ZABs as satisfactory bifunctional electrocatalysts. Table 3 lists and compares the performances of recently reported liquid ZABs based on electrospun nanofibers electrocatalysts. Due to the optimized hierarchically porous carbon microstructure of electrospun nanofibers electrocatalysts

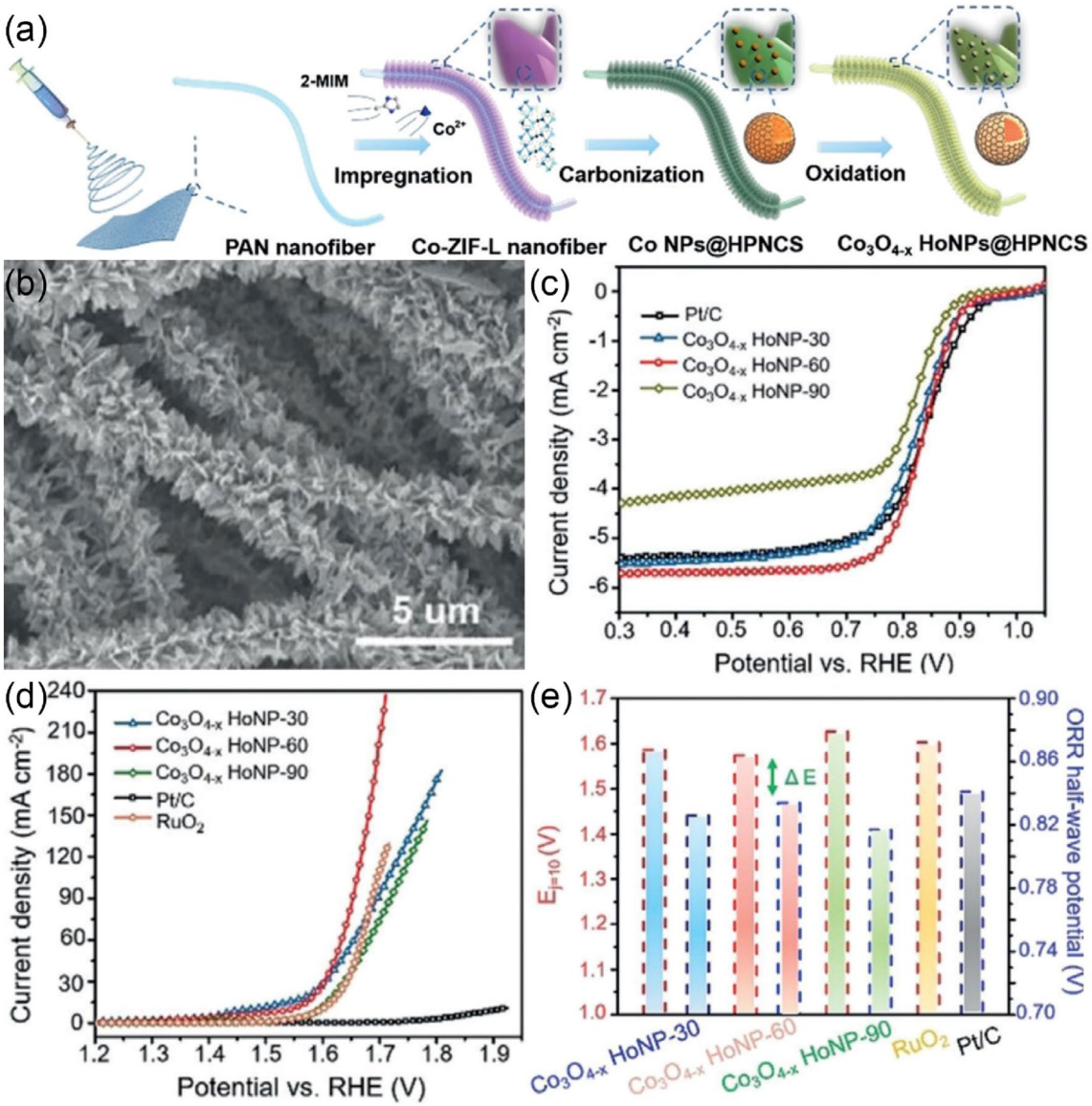

Fig. 4 **a** Illustration of the preparation process. **b** SEM image of Co_3O_{4-x}HoNPs@HPNCS. **c** ORR polarization curves of different catalysts recorded at 10 mV·s^{-1}. **d** OER polarization curves of different catalysts recorded at 5 mV·s^{-1}. **e** The potential gap (ΔE) between the $E_{1/2}$ of ORR and $E_{j=10}$ of OER for different catalysts. [17]

with a large number of active sites, and the mass activity of electrospun nanofibers electrocatalysts is better than the conventional catalysts, most liquid ZABs based on electrospun nanofibers electrocatalysts in this table demonstrate higher current density and peak density in the field of liquid ZABs. As reported in Fig. 5b–d [42], the ZABs based on CMO/S-300 exhibits a current density of 128 mA cm^{-2} (at 1.0 V) and peak density of 148 mW cm^{-2} (at 1.49 V). Furthermore, a LED screen displaying "Zn–Air" is shown as a demo. It possesses a very small voltage gap of 0.67 V and tiny diminishing after a 120 cycles stability test. Additionally, such outstanding advantages benefit from the promotion of electric conductivity and surface vacancies defect after sulfur doping engineering. In the future, the liquid ZABs based on electrospun nanofibers electrocatalysts might explore the promising practicality in energy devices.

Flexible Solid-State ZABs Based on Electrospun Nanofibers Electrocatalysts

Liquid ZABs are vulnerable to operating conditions such as excessive volume and difficulty in storage/transportation. In recent years, wearable electronic devices such as electronic watches and foldable curved surface electronic screens have rapidly entered the public view. At present, numerous investigations are focused on wearable electronic

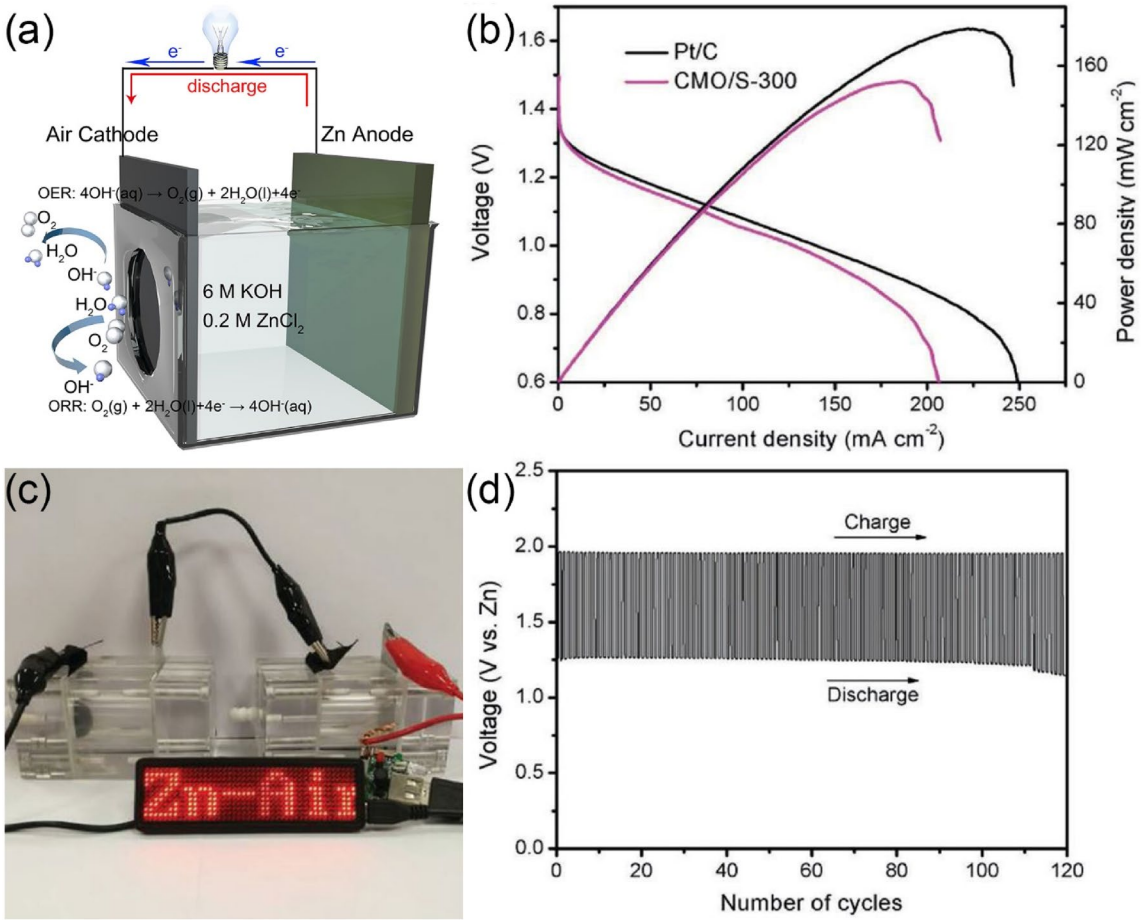

Fig. 5 **a** Schematic configuration of rechargeable liquid ZABs. **b** Polarization curves and power densities of liquid ZABs based on CMO/S-300 and Pt/C air electrode catalysts. **c** Photograph of an indicator light LED screen showing the "Zn–Air", powered by two liquid ZABs with the CMO/S air–cathode connected in series. **d** Galvanostatic pulse cycling at 5 mA cm^{-2} with a duration of 400 s per cycle of CMO/S-300 cathodes [42]

devices, especially flexible solid-state ZABs with preferable mechanical toughness and strength. As shown in Fig. 6a, the flexible ZABs are composed of a gel polymer electrolyte (GPE), cathode (same as the gas diffusion electrode of liquid ZABs), and anode (Zn foil). Additionally, the flexible electrospun nanofibers electrodes with self-supported structure maintain decent systemic efficiency and deliver adequate cycle life. Herein, some recently reported flexible solid-state ZABs based on electrospun nanofibers electrocatalysts with exceptional charge–discharge stability are compared in Table 4, most flexible solid-state ZABs based on electrospun nanofibers electrocatalysts in this table demonstrate higher current density and peak density in the field of flexible solid-state ZABs. These impressive functions such as steady cycling stability and low voltage gap in this table can be attributed to electrospun catalysts with the smallest reversible oxygen overpotential, especially the binder-free electrospun nanofibers with self-supported structure. Firstly, electrospun nanofibers with self-supported structures are easy to be directly used as working electrode for strong ion/electron diffusion without high-cost binders. Secondly, the electrode is binder-free to avoid peeling off during the electrochemical reaction, which would exhibit stable durability. Lastly, the flexibility of self-supported structure displays satisfactory battery stability of charging/discharging in different folding angle conditions. For instance, $CuCo_2S_4$ NSs@N-CNFs based solid-state ZABs display satisfactory battery stability in different folding angle conditions (Fig. 6b, c). Furthermore, they have a peak power density of 232 mW cm^{-2} and a minimal voltage gap of 0.8 V for 300 cycles (Fig. 6d, e) [41]. The remarkable bifunctional catalytic performance of $CuCo_2S_4$ nanosheets@N-doped carbon nanofiber is attributed to situ sulfurization combining electrospinning at room temperature, that scalable fabrication process optimizes the chemical composition of the catalyst surface. Consequently, it should have commercial significance to study the application of electrospun nanofibers in flexible solid-state ZABs electrodes.

Table 3 Performances of recently reported liquid ZABs based on electrospun nanofibers electrocatalysts

Catalyst	Cycling current density (mA cm^{-2})	Discharge voltage (V)	Charge voltage (V)	Voltage gap (V)	Cycling stability	References
Ni|MnO/CNF	10	1.2	2.13	0.93	350 cycles	[40]
CMO/S-300	5	1.25	1.93	0.67	120 cycles	[42]
N, F, P tri-doped CNF	10	1.25	2	0.75	200 cycles	[43]
FeCo@MNC	20	1	1.9	0.9	24 h	[46]
$NiCo_2O_4$-A_1 nanostructure	20	1.84	1.00	0.84	50 cycles	[52]
$LaNi_{0.85}Mg_{0.15}O_3$	10	1.18	2.1	0.92	110 h	[54]
CNCF-800	10	1	2	1	88 h	[58]
BSCF-80-ES	20	1.16	2.05	0.89	140 cycles	[61]
Co_3O_4/N-ACCNF	5	1.25	2	0.75	80 h	[64]
Fe/N-CNFs	10	1.24	2.21	0.97	55 h	[66]
CMS/NCNF	10	1.142	2.125	0.983	100 h	[73]
$NiCo_2O$@C	5	1.184	1.922	0.738	200 h	[74]
CCO@C	10	1.11	1.9	0.79	160 cycles	[75]
FeS_2–CoS_2/NCFs	10	1.28	2	0.72	250 h	[77]
$PrBa_{0.5}Sr_{0.5}Co_{2-x}Fe_xO_{5+\delta}$-NF	10	1.1	2.1	1.0	150 cycles	[81]
Co-N_x@CNF700	5	1.2	2.3	1.1	70 h	[82]
Co-CeO_2-N-C nanofibers	2	1.19	2.06	0.87	113 h	[84]
CMO/NCNF	10	1.21	1.98	0.77	350 cycles	[87]
NSCFs/Ni-Co-$NiCo_2O$	10	1.1	2.1	1.0	380 h	[92]
FeNi/N-CPCF-950	10	1.222	1.986	0.764	960 cycles	[93]
LCNP@NCNF	10	1.18	2.13	0.95	500 cycles	[94]
Co_9S_8/NSC nanofibers	10	1.2	2.05	0.85	500 cycles	[97]
CoP/NC-800	10	1.0	2.2	1.2	35 h	[101]
NCNF-1000	10	1.20	1.93	0.73	500 cycles	[111]
CNCo-5@Fe-2	10	–	–	–	40 h	[113]
FeCo-NCNFs-800	10	1.16	2.03	0.87	41.7 h	[115]
Zn/Co-N@PCNFs-800	10	1.1	2.1	1.0	18 h	[121]
N-Co/CNF-300-10	10	1.25	2.0	0.738	100 cycles	[122]

Conclusions, Prospects, and Challenges

While a great number of efficient energy storage devices have been applied to portable electronic devices and electric vehicles, there is an undeniable consensus that the further development of versatile, low-cost, and efficient catalysts is still important to achieve the commercial production of energy storage devices, especially in ZABs. Electrospun nanofibers have quickly become suitable bifunctional catalysts in advanced ZABs because of their large surface area, high porosity, good conductivity, and mechanical properties. One critical aspect of the research about electrospun nanofibers electrocatalyst is the development of nanofibers with hollow structure, which could indicate a larger surface area and porosity than solid structure, and then provide more active sites and improve the adsorption/desorption of oxygen. This unique structure reveals that electrospun nanofibers will have a lower OH* hydrogenation barrier and reduced ORR/OER overpotentials. Consequently, electrospun nanofibers exhibit a tremendous potential to be utilized for the zinc–air battery system. The second is mixing metals into electrospun nanofibers, it has been confirmed that there will be a synergy of the heterogeneous interface between different metals and 1D porous nanofibers, the chemical composition of the catalyst surface and coordination sites will be optimized simultaneously, which is one key to unlock substantial gains in ORR/OER performance. Therefore, electrospun nanofibers catalysts as air cathode of ZABs demonstrate a high battery capacity and a relatively high peak power density. The last is the innovation of electrospun nanofibers with self-supported structure. This innovation eliminates the disadvantages of adding binders to powder catalysts and inhibiting the coverage of active sites. The binder-free self-supported electrospun nanofibers exhibit excellent stability for battery charging/discharging processes and ORR/OER in alkaline medium. A wearable ZABs device using electrospun nanofibers as

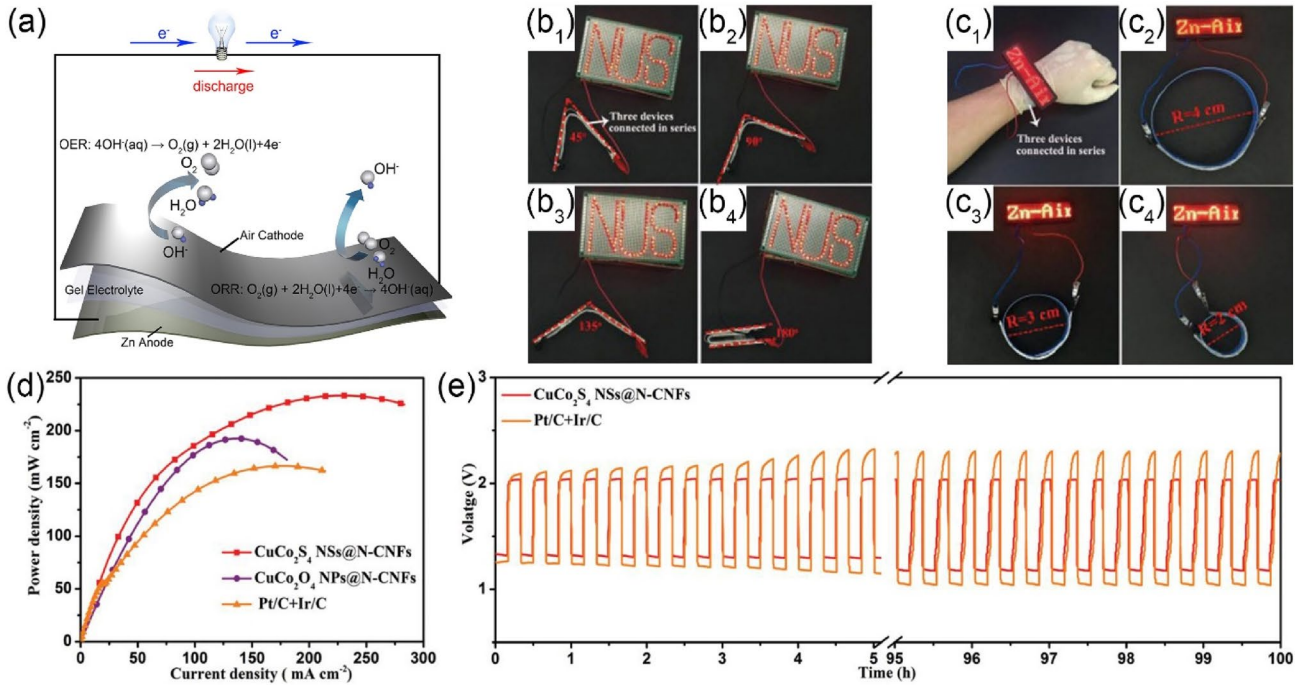

Fig. 6 **a** Schematic configuration of rechargeable flexible solid-state ZABs. Digital optical images of three flexible ZABs connected in series to power a "NUS" logo with red LEDs under $\mathbf{b_1}$–$\mathbf{b_4}$ different bending angles, $\mathbf{c_1}$–$\mathbf{c_4}$ and a "Zn–Air" logo with red LEDs different bending radius. **d** Power-current density curves, **e** comparison of the cycling stabilities of solid-state ZABs based on $CuCo_2S_4$ NSs@N-CNFs air electrode catalysts. [41]

Table 4 Performances of recently reported flexible solid-state ZABs based on electrospun nanofibers electrocatalysts

Catalyst	Cycling current density (mA cm^{-2})	Discharge voltage (V)	Charge voltage (V)	Voltage gap (V)	Cycling stability	References
$CuCo_2S_4$ NSs@N-CNFs	5	1.3	2.1	0.8	300 cycles	[41]
CMO/S-300	1	1.2	1.7	0.5	10 h	[42]
BSCF-80-ES	10	1.13	1.97	0.84	100 cycles	[61]
CMS/NCNF	5	1.2	1.93	0.73	7 h	[73]
Co-CeO_2-N-C nanofibers	1	1.00	2.08	1.08	11 h	[84]
CMO/NCNF	1	1.13	1.97	0.84	5 h	[87]
NCNF-1000	2	1.0	1.78	0.78	48 cycles	[111]
Co_3O_{4-x} HoNPs@HPNCS-60	3	1.2	1.73	0.53	50 cycles	[17]
CoNCNTF/CNF	0.5	1.21	1.50	0.29	68 cycles	[117]
Co SA@NCF/CNF	6.25	1.25	1.85	0.6	90 cycles	[34]
Co_3O_4/MWCNT	0.5	1.20	2.08	0.88	130 cycles	[123]

air electrode demonstrates battery stability as well as its high deformation tolerance. Thus, the flexible electrospun nanofibers electrodes with self-supported structures have gained popularity and significance in the fabrication of ZABs, and provide new insights into rational design of self-supported electrodes for flexible ZABs devices. In addition to metal–air batteries, electrospun nanofibers also have several novel applications in the field of energy conversion (e.g., fuel cells, solar cells, and water splitting), energy storage (e.g., metal-ion batteries), medicine (e.g., drug delivery devices and biomedical scaffolds), and environment (e.g., filter membranes).

Nevertheless, certain essential studies and massive technical problems about electrospun nanofibers are still needed to be discerned and addressed. Firstly, electrospun nanofibers with tube-in-tube structure are synthesized by a coaxial spinneret with multiple syringes with different precursor fluids loaded in the different syringes, so it's complex to make this process realized in commercial application. Secondly, the fibers from nanometers to micrometers can be prepared

by electrospinning, but it's difficult to consistently maintain the morphologies at the nanoscale such as micropores through precise control. Thirdly, there is an urgent need to develop low-cost and eco-friendly materials for green electrospinning, because the polymer precursors used for electrospinning may be expensive and detrimental to the environment (e.g., toxic, corrosive, and difficult to recycle). Fourthly, there are further investigations of electrospinning processing to be carried out, for instance, the selection of metal species loading and related polymer precursors, the temperatures of stabilization and carbonization, the commercial application of multi-jet emitters/nozzles, improving the toughness of electrospun nanofibers by synthesizing novel composite materials. Last but not least, electrospun nanofibers also need further deeply investigated in the application of ZABs, for instance, the weakness of imperfect cycle stability and the attenuation of capacity. In summary, the rational design of rich nanofibers in active sites and high porosity via electrospinning technique is still popular in advanced battery devices. Electrospun nanofibers probably create an avenue to replace precious metals catalysts in future, which will provide valuable insight in the innovation and application of ZABs based on electrospun nanofibers.

Acknowledgements This work was supported by the National Natural Science Foundation of China (51871119, 51901100, and 22101132), Jiangsu Provincial Founds for Natural Science Foundation (BK20170793, BK20180015, and BK20210311), and State Key Laboratory for Modification of Chemical Fibers and Polymer Materials, Donghua University.

Declarations

Conflict of interest The authors state that there are no conflicts of interest to disclose.

References

1. Li BQ, Zhao CX, Chen S, Liu JN, Chen X, Song L, Zhang Q. Framework-porphyrin-derived single-atom bifunctional oxygen electrocatalysts and their applications in Zn–air batteries. *Adv Mater.* **2019**;*31*:1900592.
2. Pan Y, Liu S, Sun K, Chen X, Wang B, Wu K, Cao X, Cheong WC, Shen R, Han A, Chen Z, Zheng L, Luo J, Lin Y, Liu Y, Wang D, Peng Q, Zhang Q, Chen C, Li Y. A bimetallic Zn/Fe polyphthalocyanine-derived single-atom Fe–N_4 catalytic site: a superior trifunctional catalyst for overall water splitting and Zn–air batteries. *Angew Chem Int Ed.* **2018**;57:8614.
3. Qiao Y, Yuan P, Hu Y, Zhang J, Mu S, Zhou J, Li H, Xia H, He J, Xu Q. Sulfuration of an Fe–N–C catalyst containing Fe_xC/Fe species to enhance the catalysis of oxygen reduction in acidic media and for use in flexible Zn–air batteries. *Adv Mater.* **2018**;*30*:1804504.
4. Li B-Q, Zhang S-Y, Wang B, Xia Z-J, Tang C, Zhang Q. A porphyrin covalent organic framework cathode for flexible Zn–air batteries. *Energy Environ Sci.* **2018**;*11*:1723.
5. Guan C, Sumboja A, Wu H, Ren W, Liu X, Zhang H, Liu Z, Cheng C, Pennycook SJ, Wang J. Hollow Co_3O_4 nanosphere embedded in carbon arrays for stable and flexible solid-state zinc–air batteries. *Adv Mater.* **2017**;*29*:1704117.
6. Jiang H, Gu J, Zheng X, Liu M, Qiu X, Wang L, Li W, Chen Z, Ji X, Li J. Defect-rich and ultrathin N doped carbon nanosheets as advanced trifunctional metal-free electrocatalysts for the ORR, OER and HER. *Energy Environ Sci.* **2019**;*12*:322.
7. Wu M, Zhang G, Qiao J, Chen N, Chen W, Sun S. Ultra-long life rechargeable zinc-air battery based on high-performance trimetallic nitride and NCNT hybrid bifunctional electrocatalysts. *Nano Energy.* **2019**;*61*:86.
8. Zou H, Li G, Duan L, Kou Z, Wang J. In situ coupled amorphous cobalt nitride with nitrogen-doped graphene aerogel as a trifunctional electrocatalyst towards Zn–air battery deriven full water splitting. *Appl Catal B Environ.* **2019**;*259*:118100.
9. Zhong X, Yi W, Qu Y, Zhang L, Bai H, Zhu Y, Wan J, Chen S, Yang M, Huang L, Gu M, Pan H, Xu B. Co single-atom anchored on Co_3O_4 and nitrogen-doped active carbon toward bifunctional catalyst for zinc-air batteries. *Appl Catal B Environ.* **2020**;*260*:118188.
10. Sun H, Li Q, Lian Y, Zhang C, Qi P, Mu Q, Jin H, Zhang B, Chen M, Deng Z, Peng Y. Highly efficient water splitting driven by zinc-air batteries with a single catalyst incorporating rich active species. *Appl Catal B Environ.* **2020**;*263*:118139.
11. Li Z, Lv L, Ao X, Li J-G, Sun H, An P, Xue X, Li Y, Liu M, Wang C, Liu M. An effective method for enhancing oxygen evolution kinetics of $LaMO_3$ (M = Ni Co, Mn) perovskite catalysts and its application to a rechargeable zinc–air battery. *Appl Catal B Environ.* **2020**;*262*:118291.
12. Jin Q, Ren B, Chen J, Cui H, Wang C. A facile method to conduct 3D self-supporting Co–FeCo/N-doped graphenelike carbon bifunctional electrocatalysts for flexible solid-state zinc air. *Appl Catal B Environ.* **2019**;*259*:117887.
13. Feng Q, Zhao Z, Yuan X-Z, Li H, Wang H. Oxygen vacancy engineering of yttrium ruthenate pyrochlores as an efficient oxygen catalyst for both proton exchange membrane water electrolyzers and rechargeable zinc-air batteries. *Appl Catal B Environ.* **2020**;*260*:118176.
14. Ma L, Chen S, Pei Z, Huang Y, Liang G, Mo F, Yang Q, Su J, Gao Y, Zapien JA, Zhi C. Single-site active iron-based bifunctional oxygen catalyst for a compressible and rechargeable zinc–air battery. *ACS Nano.* **1949**;*2018*:12.
15. Bôas NV, Junior JBS, Varanda LC, Machado SAS, Calegaro ML. Bismuth and cerium doped cryptomelane-type manganese dioxide nanorods as bifunctional catalysts for rechargeable alkaline metal–air batteries. *Appl Catal B Environ.* **2019**;*258*:118014.
16. Guan C, Sumboja A, Zang W, Qian Y, Zhang H, Liu X, Liu Z, Zhao D, Pennycook SJ, Wang J. Decorating Co/CoN_x nanoparticles in nitrogen-doped carbon nanoarrays for flexible and rechargeable zinc-air batteries. *Energy Storage Mater.* **2019**;*16*:243.
17. Ji D, Fan L, Tao L, Sun Y, Li M, Yang G, Tran TQ, Ramakrishna S, Guo S. The Kirkendall effect for engineering oxygen vacancy of hollow Co_3O_4 nanoparticles toward high-performance portable zinc–air batteries. *Angew Chem Int Ed.* **2019**;*58*:13840.
18. Wang H, Yuan S, Ma D, Zhang X, Yan J. Electrospun materials for lithium and sodium rechargeable batteries: from structure evolution to electrochemical performance. *Energy Environ Sci.* **2015**;*8*:1660.
19. Cao X, Deng J, Pan K. Electrospinning Janus type CoO_x/C nanofibers as electrocatalysts for oxygen reduction reaction. *Adv Fiber Mater.* **2020**;*2*:85.
20. Hu G, Zhang X, Liu X, Yu J, Ding B. Strategies in precursors and post treatments to strengthen carbon nanofibers. *Adv Fiber Mater.* **2020**;*2*:46.

21. Inagaki M, Yang Y, Kang F. Carbon nanofibers prepared via electrospinning. *Adv Mater.* **2012**;*24*:2547.
22. Wang M, Ye C, Liu H, Xu M, Bao S. Nanosized metal phosphides embedded in nitrogen-doped porous carbon nanofibers for enhanced hydrogen evolution at all pH values. *Angew Chem Int Ed.* **2018**;*57*:1963.
23. Hu G, Zhang X, Liu X, Yu J, Ding B. Electrospun nanofibers withstandable to high-temperature reactions: synergistic effect of polymer relaxation and solvent removal. *Adv Fiber Mater.* **2021**;*3*:14.
24. Kunwar R, Harilal M, Krishnan SG, Pal B, Misnon II, Mariappan CR, Ezema FI, Elim HI, Yang C-C, Jose R. Pseudocapacitive charge storage in thin nanobelts. *Adv Fiber Mater.* **2019**;*1*:205.
25. Shi Q, Sun J, Hou C, Li Y, Zhang Q, Wang H. Advanced functional fiber and smart textile. *Adv Fiber Mater.* **2019**;*1*:3.
26. Sun Y, Mwandeje JB, Wangatia LM, Zabihi F, Nedeljković J, Yang S. Enhanced photocatalytic performance of surface-modified TiO_2 nanofibers with rhodizonic acid. *Adv Fiber Mater.* **2020**;*2*:118.
27. Tebyetekerwa M, Xu Z, Yang S, Ramakrishna S. Electrospun nanofibers-based face masks. *Adv Fiber Mater.* **2020**;*2*:161.
28. Cavaliere S, Subianto S, Savych I, Jones DJ, Roziere J. Electrospinning: designed architectures for energy conversion and storage devices. *Energy Environ Sci.* **2011**;*4*:4761.
29. Yan C, Zhu P, Jia H, Zhu J, Selvan RK, Li Y, Dong X, Du Z, Angunawela I, Wu N, Dirican M, Zhang X. High-performance 3-D fiber network composite electrolyte enabled with li–ion conducting nanofibers and amorphous PEO-based cross-linked polymer for ambient all-solid-state lithium-metal batteries. *Adv Fiber Mater.* **2019**;*1*:46.
30. Su Y, Chen C, Pan H, Yang Y, Chen G, Zhao X, Li W, Gong Q, Xie G, Zhou Y, Zhang S, Tai H, Jiang Y, Chen J. Muscle fibers inspired high-performance piezoelectric textiles for wearable physiological monitoring. *Adv Funct Mater.* **2021**;*31*:2010962.
31. Su Y, Li W, Yuan L, Chen C, Pan H, Xie G, Conta G, Ferrier S, Zhao X, Chen G, Tai H, Jiang Y, Chen J. Piezoelectric fiber composites with polydopamine interfacial layer for self-powered wearable biomonitoring. *Nano Energy.* **2021**;*89*:106321.
32. Zeng S, Chen H, Wang H, Tong X, Chen M, Di J, Li Q. Crosslinked carbon nanotube aerogel films decorated with cobalt oxides for flexible rechargeable Zn–air batteries. *Small.* **2017**;*13*:1700518.
33. Li L, Peng S, Lee JKY, Ji D, Srinivasan M, Ramakrishna S. Electrospun hollow nanofibers for advanced secondary batteries. *Nano Energy.* **2017**;*39*:111.
34. Ji D, Fan L, Li L, Peng S, Yu D, Song J, Ramakrishna S, Guo S. Atomically transition metals on self-supported porous carbon flake arrays as binder-free air cathode for wearable zinc–air batteries. *Adv Mater.* **2019**;*31*:1808267.
35. Li Y, Zhong C, Liu J, Zeng X, Qu S, Han X, Deng Y, Hu W, Lu J. Atomically thin mesoporous Co_3O_4 layers strongly coupled with N-rGO nanosheets as high-performance bifunctional catalysts for 1D knittable zinc–air batteries. *Adv Mater.* **2017**;*30*:1703657.
36. Thavasi V, Singh G, Ramakrishna S. Electrospun nanofibers in energy and environmental applications. *Energy Environ Sci.* **2008**;*1*:205.
37. Chakraborty S, Liao IC, Adler A, Leong KW. Electrohydrodynamics: a facile technique to fabricate drug delivery systems. *Adv Drug Deliv Rev.* **2009**;*61*:1043.
38. Li Y, Dai H. Recent advances in zinc–air batteries. *Chem Soc Rev.* **2014**;*43*:5257.
39. Tang C, Wang B, Wang HF, Zhang Q. Defect engineering toward atomic Co–N_x–C in hierarchical graphene for rechargeable flexible solid Zn–air batteries. *Adv Mater.* **2017**;*29*:1703185.
40. Ji D, Sun J, Tian L, Chinnappan A, Zhang T, Jayathilaka WADM, Gosh R, Baskar C, Zhang Q, Ramakrishna S. Engineering of the heterointerface of porous carbon nanofiber-supported nickel and manganese oxide nanoparticle for highly efficient bifunctional oxygen catalysis. *Adv Funct Mater.* **2020**;*30*:1910568.
41. Pan Z, Chen H, Jie Yang YM, Zhang Q, Kou Z, Ding X, Pang Y, Zhang L, Gu Q, Yan C, Wang J. $CuCo_2S_4$ Nanosheets@N-doped carbon nanofibers by sulfurization at room temperature as bifunctional electrocatalysts in flexible quasi-solid-state Zn–air batteries. *Adv Sci.* **2019**;*6*:1900628.
42. Peng S, Han X, Li L, Chou S, Ji D, Huang H, Du Y, Liu J, Ramakrishna S. Electronic and defective engineering of electrospun $CaMnO_3$ nanotubes for enhanced oxygen electrocatalysis in rechargeable zinc–air batteries. *Adv Energy Mater.* **2018**;*8*:1800612.
43. Wu M, Wang Y, Wei Z, Wang L, Zhuo M, Zhang J, Han X, Ma J. Ternary doped porous carbon nanofibers with excellent ORR and OER performance for zinc-air batteries. *J Mater Chem A.* **2018**;*6*:10918.
44. Chen H, Wang N, Di J, Zhao Y, Song Y, Jiang L. Nanowire-in-microtube structured core/shell fibers via multifluidic coaxial electrospinning. *Langmuir.* **2010**;*26*:11291.
45. Zhang G, Xia BY, Xiao C, Yu L, Wang X, Xie Y, Lou XW. General formation of complex tubular nanostructures of metal oxides for the oxygen reduction reaction and lithium-ion batteries. *Angew Chem Int Ed.* **2013**;*52*:8643.
46. Li C, Wu M, Liu R. High-performance bifunctional oxygen electrocatalysts for zinc-air batteries over mesoporous Fe/Co–N–C nanofibers with embedding FeCo alloy nanoparticles. *Appl Catal B Environ.* **2019**;*244*:150.
47. Fu Y, Yu H-Y, Jiang C, Zhang T-H, Zhan R, Li X, Li J-F, Tian J-H, Yang R. NiCo alloy nanoparticles decorated on N-doped carbon nanofibers as highly active and durable oxygen electrocatalyst. *Adv Funct Mater.* **2018**;*28*:1705094.
48. Surendran S, Shanmugapriya S, Sivanantham A, Shanmugam S, Kalai SR. Electrospun carbon nanofibers encapsulated with NiCoP: a multifunctional electrode for supercapattery and oxygen reduction, oxygen evolution, and hydrogen evolution reactions. *Adv Funct Mater.* **2018**;*8*:1800555.
49. Yu A, Lee C, Lee NS, Kim MH, Lee Y. Highly efficient silver–cobalt composite nanotube electrocatalysts for favorable oxygen reduction reaction. *ACS Appl Mater Interfaces.* **2016**;*8*:32833.
50. Yu A, Lee C, Kim MH, Lee Y. Nanotubular iridium–cobalt mixed oxide crystalline architectures inherited from cobalt oxide for highly efficient oxygen evolution reaction catalysis. *ACS Appl Mater Interfaces.* **2017**;*9*:35057.
51. Lee Y-G, Ahn H-J. Tri(Fe/N/F)-doped mesoporous carbons as efficient electrocatalysts for the oxygen reduction reaction. *Appl Surf Sci.* **2019**;*487*:389.
52. Prabu M, Ketpang K, Shanmugam S. Hierarchical nanostructured $NiCo_2O_4$ as an efficient bifunctional non-precious metal catalyst for rechargeable zinc–air batteries. *Nanoscale.* **2014**;*6*:3173.
53. Wei P, Sun X, Liang Q, Li X, He Z, Hu X, Zhang J, Wang M, Li Q, Yang H, Han J, Huang Y. Enhanced oxygen evolution reaction activity by encapsulating NiFe alloy nanoparticles in nitrogen-doped carbon nanofibers. *ACS Appl Mater Interfaces.* **2020**;*12*:31503.
54. Bian J, Su R, Yao Y, Wang J, Zhou J, Li F, Wang ZL, Sun C. Mg doped perovskite $LaNiO_3$ nanofibers as an efficient bifunctional catalyst for rechargeable zinc–air batteries. *ACS Appl Energy Mater.* **2019**;*2*:923.
55. Mooste M, Kibena-Põldsepp E, Vassiljeva V, Kikas A, Käärik M, Kozlova J, Kisand V, Külaviir M, Cavaliere S, Leis J, Krumme A, Sammelselg V, Holdcroft S, Tammeveski K. Electrospun polyacrylonitrile-derived Co or Fe containing nanofibre catalysts

for oxygen reduction reaction at the alkaline membrane fuel cell cathode. *ChemCatChem.* **2020**;*12*:4568.
56. Li M, Wang H, Zhu W, Li W, Wang C, Lu X. RuNi nanoparticles embedded in N-doped carbon nanofibers as a robust bifunctional catalyst for efficient overall water splitting. *Adv Sci.* **2020**;*7*:1901833.
57. Jiménez-Morales I, Haidar F, Cavaliere S, Jones D, Rozière J. Strong interaction between platinum nanoparticles and tantalum-doped tin oxide nanofibers and its activation and stabilization effects for oxygen reduction reaction. *ACS Catal.* **2020**;*10*:10399.
58. Li H, An M, Zhao Y, Pi S, Li C, Sun W, Wang H-G. Co nanoparticles encapsulated in N-doped carbon nanofibers as bifunctional catalysts for rechargeable Zn–air battery. *Appl Surf Sci.* **2019**;*478*:560.
59. Lee C-H, Park H-N, Lee Y-K, Chung YS, Lee S, Joh H-I. Palladium on yttrium-embedded carbon nanofibers as electrocatalyst for oxygen reduction reaction in acidic media. *Electrochem Commun.* **2019**;*106*:106516.
60. Zhao Y, Zhang J, Guo X, Fan H, Wu W, Liu H, Wang G. Fe_3C@ nitrogen doped CNT arrays aligned on nitrogen functionalized carbon nanofibers as highly efficient catalysts for the oxygen evolution reaction. *J Mater Chem A.* **2017**;*5*:19672.
61. Wu X, Miao H, Hu R, Chen B, Yin M, Zhang H, Xia L, Zhang C, Yuan J. A-site deficient perovskite nanofibers boost oxygen evolution reaction for zinc–air batteries. *Appl Surf Sci.* **2021**;*536*:147806.
62. Zhang C-L, Lu B-R, Cao F-H, Wu Z-Y, Zhang W, Cong H-P, Yu S-H. Electrospun metal-organic framework nanoparticle fibers and their derived electrocatalysts for oxygen reduction reaction. *Nano Energy.* **2019**;*55*:226.
63. Miao Y-E, Yan J, Ouyang Y, Lu H, Lai F, Wu Y, Liu T. A bio-inspired N-doped porous carbon electrocatalyst with hierarchical superstructure for efficient oxygen reduction reaction. *Appl Surf Sci.* **2018**;*443*:266.
64. Qiu L, Han X, Lu Q, Zhao J, Wang Y, Chen Z, Zhong C, Hu W, Deng Y. Co_3O_4 nanoparticles supported on N-doped electrospinning carbon nanofibers as an efficient and bifunctional oxygen electrocatalyst for rechargeable Zn–air batteries. *Inorg Chem Front.* **2019**;*6*:3554.
65. An X, Shin D, Jeong J, Lee J. Metal-derived mesoporous structure of a carbon nanofiber electrocatalyst for improved oxygen evolution reaction in alkaline water electrolysis. *ChemElectroChem.* **2016**;*3*:1720.
66. Deng D, Tian Y, Li H, Li H, Xu L, Qian J, Li H, Zhang Q. Electrospun Fe, N co-doped porous carbon nanofibers with Fe_4N species as a highly efficient oxygen reduction catalyst for rechargeable zinc–air batteries. *Appl Surf Sci.* **2019**;*492*:417.
67. Hyun S, Ahilan V, Kim H, Shanmugam S. The influence of $Co_3V_2O_8$ morphology on the oxygen evolution reaction activity and stability. *Electrochem Commun.* **2016**;*63*:44.
68. Ding Z, Cheng Q, Zou L, Fang J, Zou Z, Yang H. Controllable synthesis of titanium nitride nanotubes by coaxial electrospinning and their application as a durable support for oxygen reduction reaction electrocatalysts. *Chem Commun.* **2017**;*53*:13233.
69. Li Z, Li J-G, Ao X, Sun H, Wang H, Yuen M-F, Wang C. Conductive metal–organic frameworks endow high-efficient oxygen evolution of $La_{0.6}Sr_{0.4}Co_{0.8}Fe_{0.2}O_3$ perovskite oxide nanofibers. *Electrochim Acta.* **2020**;*334*:135638.
70. Li B, Sasikala SP, Kim DH, Bak J, Kim I-D, Cho E, Kim SO. Fe–N_4 complex embedded free-standing carbon fabric catalysts for higher performance ORR both in alkaline & acidic media. *Nano Energy.* **2019**;*56*:524.
71. Deng X, Yin S, Wu X, Sun M, Xie Z, Huang Q. Synthesis of PtAu/TiO_2 nanowires with carbon skin as highly active and highly stable electrocatalyst for oxygen reduction reaction. *Electrochim Acta.* **2018**;*283*:987.
72. Li T, Lv Y, Su J, Wang Y, Yang Q, Zhang Y, Zhou J, Xu L, Sun D, Tang Y. Anchoring $CoFe_2O_4$ nanoparticles on N-doped carbon nanofibers for high-performance oxygen evolution reaction. *Adv Sci.* **2017**;*4*:1700226.
73. Wang Y, Fu J, Zhang Y, Li M, Hassan FM, Li G, Chen Z. Continuous fabrication of a MnS/Co nanofibrous air electrode for wide integration of rechargeable zinc–air batteries. *Nanoscale.* **2017**;*9*:15865.
74. Liu C, Zuo P, Jin Y, Zong X, Li D, Xiong Y. Defect-enriched carbon nanofibers encapsulating NiCo oxide for efficient oxygen electrocatalysis and rechargeable Zn–air batteries. *J Power Sources.* **2020**;*473*:228604.
75. Wang X, Li Y, Jin T, Meng J, Jiao L, Zhu M, Chen J. Electrospun thin-walled $CuCo_2O_4$@C nanotubes as bifunctional oxygen electrocatalysts for rechargeable Zn–air batteries. *Nano Lett.* **2017**;*17*:7989.
76. Hassen D, Shenashen MA, El-Safty SA, Selim MM, Isago H, Elmarakbi A, El-Safty A, Yamaguchi H. Nitrogen-doped carbon-embedded TiO_2 nanofibers as promising oxygen reduction reaction electrocatalysts. *J Power Sources.* **2016**;*330*:292.
77. Shi X, He B, Zhao L, Gong Y, Wang R, Wang H. FeS_2–CoS_2 incorporated into nitrogen-doped carbon nanofibers to boost oxygen electrocatalysis for durable rechargeable Zn–air batteries. *J Power Sources.* **2021**;*482*:228955.
78. Wei Z, Ren Y, Zhao H, Wang M, Tang H. Controllable preparation and synergistically improved catalytic performance of TiC/C hybrid nanofibers via electrospinning for the oxygen reduction reaction. *Ceram Int.* **2020**;*46*:25313.
79. Li T, Li S, Liu Q, Tian Y, Zhang Y, Fu G, Tang Y. Hollow Co_3O_4/CeO_2 heterostructures in situ embedded in N-doped carbon nanofibers enable outstanding oxygen evolution. *ACS Sustain Chem Eng.* **2019**;*7*:17950.
80. Liu T, Cai S, Gao Z, Liu S, Li H, Chen L, Li M, Guo H. Facile synthesis of the porous FeCo@nitrogen-doped carbon nanosheets as bifunctional oxygen electrocatalysts. *Electrochim Acta.* **2020**;*335*:135647.
81. Bu Y, Gwon O, Nam G, Jang H, Kim S, Zhong Q, Cho J, Kim G. A highly efficient and robust cation ordered perovskite oxide as a bifunctional catalyst for rechargeable zinc–air batteries. *ACS Nano.* **2017**;*11*:11594.
82. Yoon KR, Choi J, Cho S-H, Jung J-W, Kim C, Cheong JY, Kim I-D. Facile preparation of efficient electrocatalysts for oxygen reduction reaction: one-dimensional meso/macroporous cobalt and nitrogen Co-doped carbon nanofibers. *J Power Sources.* **2018**;*380*:174.
83. Xia H, Zhang S, Zhu X, Xing H, Xue Y, Huang B, Sun M, Li J, Wang E. Highly efficient catalysts for oxygen reduction using well-dispersed iron carbide nanoparticles embedded in multi-channel hollow nanofibers. *J Mater Chem A.* **2020**;*8*:18125.
84. Zhang Z, Gao D, Xue D, Liu Y, Liu P, Zhang J, Qian J. Co and CeO_2 co-decorated N-doping carbon nanofibers for rechargeable Zn–air batteries. *Nanotechnology.* **2019**;*30*:395401.
85. Wang M, Zhang C, Meng T, Pu Z, Jin H, He D, Zhang J, Mu S. Iron oxide and phosphide encapsulated within N, P-doped microporous carbon nanofibers as advanced tri-functional electrocatalyst toward oxygen reduction/evolution and hydrogen evolution reactions and zinc–air batteries. *J Power Sources.* **2019**;*413*:367.
86. Liu C, Wang J, Li J, Liu J, Wang C, Sun X, Shen J, Han W, Wang L. Electrospun ZIF-based hierarchical carbon fiber as an efficient electrocatalyst for the oxygen reduction reaction. *J Mater Chem A.* **2017**;*5*:1211.
87. Chen X, Yan Z, Yu M, Sun H, Liu F, Zhang Q, Cheng F, Chen J. Spinel oxide nanoparticles embedded in nitrogen-doped carbon nanofibers as a robust and self-standing bifunctional oxygen cathode for Zn–air batteries. *J Mater Chem A.* **2019**;*7*:24868.

88. Sankar SS, Karthick K, Sangeetha K, Gill RS, Kundu S. Annexation of nickel vanadate ($Ni_3V_2O_8$) nanocubes on nanofibers: an excellent electrocatalyst for water oxidation. *ACS Sustain Chem Eng.* **2020**;*8*:4572.
89. Wang Y, Li G, Jin J, Yang S. Hollow porous carbon nanofibers as novel support for platinum-based oxygen reduction reaction electrocatalysts. *Int J Hydrog Energy.* **2017**;*42*:5938.
90. Kim SY, Yu A, Lee Y, Kim HY, Kim YJ, Lee NS, Lee C, Lee Y, Kim MH. Single phase of spinel Co_2RhO_4 nanotubes with remarkably enhanced catalytic performance for the oxygen evolution reaction. *Nanoscale.* **2019**;*11*:9287.
91. Niu Q, Guo J, Chen B, Nie J, Guo X, Ma G. Bimetal-organic frameworks/polymer core-shell nanofibers derived heteroatom-doped carbon materials as electrocatalysts for oxygen reduction reaction. *Carbon.* **2017**;*114*:250.
92. Liu C, Wang Z, Zong X, Jin Y, Li D, Xiong Y, Wu G. N & S co-doped carbon nanofiber network embedded with ultrafine NiCo nanoalloy for efficient oxygen electrocatalysis and Zn–air batteries. *Nanoscale.* **2020**;*12*:9581.
93. Wang Z, Ang J, Liu J, Ma XYD, Kong J, Zhang Y, Yan T, Lu X. FeNi alloys encapsulated in N-doped CNTs-tangled porous carbon fibers as highly efficient and durable bifunctional oxygen electrocatalyst for rechargeable zinc–air battery. *Appl Catal B Environ.* **2020**;*263*:118344.
94. Lin H, Xie J, Zhang Z, Wang S, Chen D. Perovskite nanoparticles@N-doped carbon nanofibers as robust and efficient oxygen electrocatalysts for Zn–air batteries. *J Colloid Interfaces Sci.* **2021**;*581*:374.
95. Ding W, Zhu H, Lu L, Zhang J, Yu H, Zhao H. Three-dimensional layered Fe–N/C catalysts built by electrospinning and the comparison of different active species on oxygen reduction reaction performance. *J Alloys Compd.* **2020**;*848*:156605.
96. Bai Q, Shen FC, Li SL, Liu J, Dong LZ, Wang ZM, Lan YQ. Cobalt@nitrogen-doped porous carbon fiber derived from the electrospun fiber of bimetal-organic framework for highly active oxygen reduction. *Small Methods.* **2018**;*2*:1800049.
97. Zheng W, Lv J, Zhang H, Zhang H-X, Zhang J. Co_9S_8 integrated into nitrogen/sulfur dual-doped carbon nanofibers as an efficient oxygen bifunctional electrocatalyst for Zn–air batteries. *Sustain Energy Fuels.* **2020**;*4*:1093.
98. Liu T, Li M, Bo X, Zhou M. Designing iron carbide embedded isolated boron (B) and nitrogen (N) atoms co-doped porous carbon fibers networks with tiny amount of BN bonds as high-efficiency oxygen reduction reaction catalysts. *J Colloid Interface Sci.* **2019**;*533*:709.
99. Guo J, Gao M, Nie J, Yin F, Ma G. ZIF-67/PAN-800 bifunctional electrocatalyst derived from electrospun fibers for efficient oxygen reduction and oxygen evolution reaction. *J Colloid Interface Sci.* **2019**;*544*:112.
100. Su J, Zang J, Tian P, Zhou S, Liu X, Li R, Wang Y, Dong L. Fe–N–Si tri-doped carbon nanofibers for efficient oxygen reduction reaction in alkaline and acidic media. *Int J Hydrog Energy.* **2020**;*45*:28792.
101. Feng L, Ding R, Chen Y, Wang J, Xu L. Zeolitic imidazolate framework-67 derived ultra-small CoP particles incorporated into N-doped carbon nanofiber as efficient bifunctional catalysts for oxygen reaction. *J Power Sources.* **2020**;*452*:227837.
102. Liu C, Wang J, Li J, Luo R, Sun X, Shen J, Han W, Wang L. Fe/N decorated mulberry-like hollow mesoporous carbon fibers as efficient electrocatalysts for oxygen reduction reaction. *Carbon.* **2017**;*114*:706.
103. Yin D, Han C, Bo X, Liu J, Guo L. Prussian blue analogues derived iron-cobalt alloy embedded in nitrogen-doped porous carbon nanofibers for efficient oxygen reduction reaction in both alkaline and acidic solutions. *J Colloid Interface Sci.* **2019**;*533*:578.
104. Xie D, Yang G, Yu D, Hao Y, Han S, Cheng Y, Hu F, Li L, Wei H, Ji C, Peng S. MoS_2 nanosheets functionalized multichannel hollow Mo_2N/carbon nanofibers as a robust bifunctional catalyst for water electrolysis. *ACS Sustain Chem Eng.* **2020**;*8*:14179.
105. Liu L, Liu H, Sun X, Li C, Bai J. Efficient electrocatalyst of Pt–Fe/CNFs for oxygen reduction reaction in alkaline media. *Int J Hydrog Energy.* **2020**;*45*:15112.
106. Wei B, Xu G, Hei J, Zhang L, Huang T. PBA derived FeCoP nanoparticles decorated on NCNFs as efficient electrocatalyst for water splitting. *Int J Hydrog Energy.* **2021**;*46*:2225.
107. Shanmugapriya S, Zhu P, Yan C, Asiri AM, Zhang X, Selvan RK. Multifunctional high-performance electrocatalytic properties of Nb_2O_5 incorporated carbon nanofibers as Pt support catalyst. *Adv Mater Interfaces.* **2019**;*6*:1900565.
108. Mo Q, Zhang W, He L, Yu X, Gao Q. Bimetallic $Ni_{2-x}Co_xP$/N-doped carbon nanofibers: solid-solution-alloy engineering toward efficient hydrogen evolution. *Appl Catal B Environ.* **2019**;*244*:620.
109. Wang Z, Li M, Fan L, Han J, Xiong Y. Fe/Ni-N-CNFs electrochemical catalyst for oxygen reduction reaction/oxygen evolution reaction in alkaline media. *Appl Surf Sci.* **2017**;*401*:89.
110. Zhu Y, Zhou W, Zhong Y, Bu Y, Chen X, Zhong Q, Liu M, Shao Z. A perovskite nanorod as bifunctional electrocatalyst for overall water splitting. *Adv Energy Mater.* **2017**;*7*:1602122.
111. Liu Q, Wang Y, Dai L, Yao J. Scalable fabrication of nanoporous carbon fiber films as bifunctional catalytic electrodes for flexible Zn–air batteries. *Adv Mater.* **2016**;*28*:3000.
112. Zhen D, Zhao B, Shin H-C, Bu Y, Ding Y, He G, Liu M. Electrospun porous perovskite $La_{0.6}Sr_{0.4}Co_{1-x}Fe_xO_{3-\delta}$ nanofibers for efficient oxygen evolution reaction. *Adv Mater Interfaces.* **2017**;*4*:1700146.
113. Zhang C-L, Liu J-T, Li H, Qin L, Cao F-H, Zhang W. The controlled synthesis of Fe_3C/Co/N-doped hierarchically structured carbon nanotubes for enhanced electrocatalysis. *Appl Catal B Environ.* **2020**;*261*:118224.
114. Li W, Li M, Wang C, Wei Y, Lu X. Fe doped CoO/C nanofibers towards efficient oxygen evolution reaction. *Appl Surf Sci.* **2020**;*506*:144680.
115. Yang L, Feng S, Xu G, Wei B, Zhang L. Electrospun MOF-based FeCo nanoparticles embedded in nitrogen-doped mesoporous carbon nanofibers as an efficient bifunctional catalyst for oxygen reduction and oxygen evolution reactions in zinc–air batteries. *ACS Sustain Chem Eng.* **2019**;*7*:5462.
116. Patil B, Satilmis B, Khalily MA, Uyar T. Atomic layer deposition of NiOOH/$Ni(OH)_2$ on PIM-1-based N-doped carbon nanofibers for electrochemical water splitting in alkaline medium. *Chemsuschem.* **2019**;*12*:1469.
117. Ji D, Fan L, Li L, Mao N, Qin X, Peng S, Ramakrishna S. Hierarchical catalytic electrodes of cobalt-embedded carbon nanotube/carbon flakes arrays for flexible solid-state zinc-air batteries. *Carbon.* **2019**;*142*:379.
118. Sankar SS, Karthick K, Sangeetha K, Kundu S. In situ modified nitrogen-enriched ZIF-67 incorporated ZIF-7 nanofiber: an unusual electrocatalyst for water oxidation. *Inorg Chem.* **2019**;*58*:13826.
119. Zhang L, Guo Q, Pitcheri R, Fu Y, Li J, Qiu Y. Silver nanofibers with controllable microstructure and crystal facet as highly efficient and methanol-tolerant oxygen reduction electrocatalyst. *J Power Sources.* **2019**;*413*:233.
120. Chen J, Chen J, Yu D, Zhang M, Zhu H, Du M. Carbon nanofiber-supported PdNi alloy nanoparticles as highly efficient bifunctional catalysts for hydrogen and oxygen evolution reactions. *Electrochim Acta.* **2017**;*246*:17.
121. Niu Q, Chen B, Guo J, Nie J, Guo X, Ma G. Flexible, porous, and metal-heteroatom-doped carbon nanofibers as efficient

ORR electrocatalysts for Zn–air battery. *Nano Micro Lett.* **2019**;*11*:147.
122. Rao P, Cui P, Wei Z, Wang M, Ma J, Wang Y, Zhao X. Integrated N–Co/carbon nanofiber cathode for highly efficient zinc–air batteries. *ACS Appl Mater Interfaces.* **2019**;*11*:29708.
123. Lee D, Kim HW, Kim JM, Kim KH, Lee SY. Flexible/rechargeable Zn–air batteries based on multifunctional heteronanomat architecture. *ACS Appl Mater Interfaces.* **2018**;*10*:22210.

Yanan Hao is working as a doctoral student in College of Materials Science and Technology, Nanjing University of Aeronautics and Astronautics. His main research interests focus on the development of novel catalysts for metalair battery and CO2 reduction.

Feng Hu is working as an associate professor in College of Materials Science and Technology, Nanjing University of Aeronautics and Astronautics. His main research interests focus on the development of novel catalysts for electrochemical water splitting and CO2 reduction.

Ying Chen is currently an MSc candidate in physical chemistry at Nanjing University of Aeronautics and Astronautics. Her research focuses on the development of excellent electrocatalytic carbon dioxide reduction catalyst materials.

Yonghan Wang is currently an MSc candidate in physical chemistry at Nanjing University of Aeronautics and Astronautics. His research focuses on the development of excellent electrocatalytic carbon dioxide reduction catalyst materials.

Jianjun Xue works as a professor in College of Materials Science and Technology, Nanjing University of Aeronautics and Astronautics. His main research interests focus on electrochemical synthesis and waste treatment and recycling.

Shengyuan Yang is an associate professor in the College of Materials Science and Engineering, Donghua University and the vice director of DHU International Cooperation Office. His research is centered in novel applications of electrospun nanomaterials like wearable electronics.

Shengjie Peng received his PhD degree in Nankai University (P.R. China) in 2010. Following postdoctoral fellow with Prof. Qingyu Yan and Prof. Seeram Ramakrishna in Nanyang Technological University and National University of Singapore, he is now working as a full professor in Nanjing University of Aeronautics and Astronautics. He has co-authored over 130 peer-reviewed publications. His current research interests focus on functional nanomaterials especially 1D structures in electrochemical catalysis and storage.

Authors and Affiliations

Yanan Hao[1] · Feng Hu[1] · Ying Chen[1] · Yonghan Wang[1] · Jianjun Xue[1] · Shengyuan Yang[2] · Shengjie Peng[1,2]

✉ Feng Hu
fenghu@nuaa.edu.cn

✉ Shengjie Peng
pengshengjie@nuaa.edu.cn

[1] College of Materials Science and Technology, Nanjing University of Aeronautics and Astronautics, Nanjing 210016, People's Republic of China

[2] State Key Laboratory for Modification of Chemical Fibers and Polymer Materials, College of Materials Science and Engineering, Donghua University, 2999 North Renmin Road, Shanghai 201620, People's Republic of China